Journal of Molecular Catalysis A: Chemical 315 (2010) 163–170

Contents lists available at ScienceDirect

Journal of Molecular Catalysis A: Chemical

journal homepage: www.elsevier.com/locate/molcata

Support effects and catalytic trends for water gas shift activity of transition metals

A. Boisen[a,b,*], T.V.W. Janssens[a], N. Schumacher[b], I. Chorkendorff[b], S. Dahl[a,*]

[a] Haldor Topsoe A/S, Nymøllevej 55, DK-2800 Kgs. Lyngby, Denmark
[b] Center for Individual Nanoparticle Functionality (CINF) and Department of Physics, Technical University of Denmark, Building 312, DK-2800 Kgs. Lyngby, Denmark

ARTICLE INFO

Article history:
Available online 26 June 2009

Keywords:
Water gas shift
Transition metals
Catalytic activity trends
Support effect

ABSTRACT

Water gas shift activity measurements for 12 transition metals (Fe, Co, Ni, Cu, Ru, Rh, Pd, Ag, Re, Ir, Pt, Au) supported on inert $MgAl_2O_4$ and $Ce_{0.75}Zr_{0.25}O_2$ are presented, to elucidate the influence of the active metal and the support. The activity is related to the adsorption energy of molecular CO and atomic oxygen on the metal; the latter is a good measure for the reactivity of the metal towards H_2O. Generally, the activity of the catalysts with the $Ce_{0.75}Zr_{0.25}O_2$ support is higher, compared to the corresponding $MgAl_2O_4$-supported catalysts. Exceptions are Cu and Au, which have a higher activity on the $MgAl_2O_4$ support and are both characterized by weak CO adsorption. For the $MgAl_2O_4$-supported catalysts a volcano-type relation between the activity and the adsorption energy of atomic oxygen on the metal is obtained. The maximum activity is found for metals with a binding energy of oxygen around −2.5 eV. No clear correlation exists with the adsorption energy of CO. In contrast, the activity for the $Ce_{0.75}Zr_{0.25}O_2$ support increases with increasing adsorption strength for CO, and based on a relatively low activity of Cu the activity does not seem to depend on the adsorption energy of oxygen. Such a change in activity-descriptor for the different supports can be rationalized by the possibility that water dissociation occurs on the redox-active $Ce_{0.75}Zr_{0.25}O_2$ support, whereas the $MgAl_2O_4$ support is inactive.

1. Introduction

The production of pure hydrogen is essential for, e.g. ammonia production and power generation by hydrogen-based low-temperature fuel cell technology. At present, hydrogen is generally produced by steam reforming or partial oxidation of methane or other carbonaceous feed stocks, which yields gas mixtures containing significant amounts of CO. The water gas shift (WGS) reaction

$$CO(g) + H_2O(g) \leftrightarrows CO_2(g) + H_2(g) \quad (1)$$

is commonly applied to purify the hydrogen. Possible on-board reforming of fuels in connection with fuel cell-powered vehicles has created a renewed interest in WGS catalysts. A high and stable water gas shift activity is crucial in this application, since it allows both for a lower reaction temperature, which favors the conversion of carbon monoxide and the production of hydrogen, and for a reduction of the size of the fuel processor [1].

Traditionally, Cu based catalysts are used for WGS at temperatures below 300 °C and iron oxide based catalysts for WGS at higher temperatures, because iron oxide is more stable towards sintering than Cu [2]. Some other supported transition metals are known to be active for the WGS reaction as well [3–11] and it is conceivable that improved WGS catalysts can be obtained by using another metal or an appropriate alloy catalyst.

In order to contribute to the fundamental understanding of a catalytic reaction over different metals it is useful to correlate the activity with easily accessible chemical and physical properties of the active metal in the catalyst. Such understandings of the catalytic trends contribute to the understanding of the reaction and can help to the identification of catalyst systems with a potentially higher activity. By example, for the methanation [12] and ammonia synthesis reactions [13], such correlations were helpful in the development of new catalysts. In the case of WGS over different transition metals, Grenoble et al. found that a volcano-type relation between the water gas shift activity of alumina supported metal catalysts and the strength of interaction of molecular CO on the metal [14] with the optimum around Cu. This type of correlation is a reflection of the principle of Sabatier which states that the optimal catalyst binds adsorbates moderately to the surface. With a too weak adsorption, the reaction rate will be low due to a low coverage of reaction intermediates (and/or too low reactivity to activate some of the reactants). Conversely, with a too strong adsorption, it is difficult to release reaction products into the gas phase, and the rate is low due to the lack of free adsorption sites on the surface [15].

* Corresponding authors. Current address: Technical University of Denmark, Department of Physics, Building 312, DK-2800 Kgs. Lyngby, Denmark.
E-mail address: soren.dahl@fysik.dtu.dk (S. Dahl).

1381-1169/$ – see front matter © 2009 Elsevier B.V. All rights reserved.
doi:10.1016/j.molcata.2009.06.019

Schumacher et al. [16] used a kinetic modeling approach to suggest that both the adsorption energy of carbon monoxide and atomic oxygen on metal surfaces are required as descriptors to adequately describe the water gas shift activity of a number of transition metal catalysts. This was done by extending the microkinetic model proposed by Ovesen et al. [17] for Cu to other metals. The description is based on the observation that all relevant adsorption and activation energies that are required in the microkinetic model correlate linearly with either the adsorption energy of CO or that of O. Hence, in this description, the adsorption energy of CO and O should not only be interpreted literally, but also as two parameters with a broader meaning. In particular, the adsorption energy of O, E_O, can be interpreted as the general reactivity of a metal, e.g. the ability to activate water [18]. The adsorption energy of CO, E_{CO}, is important, because the CO coverage can be high on metals with a strong CO adsorption, which may block the active sites and inhibit the WGS reaction. The two parameters were recently successfully used to describe the trends for catalytic CO oxidation, a reaction that also involves activation of CO and a molecule mainly interacting with the surface though oxygen atoms [19].

New insights about the WGS reaction on Cu and Pt-based catalysts were recently obtained through a combination of DFT calculations, microkinetic modeling, and experimental studies [20,21]. The reaction mechanism was found to be similar on the two metals. Extraction of the first H from water is a slow and the subsequent reaction of CO and OH results in a carboxyl (COOH) intermediate which decomposes into CO_2 and H. CO_2 formation through the surface redox step CO + O was found to be negligible. For both metals the reaction step COOH + OH = CO_2 + H_2O was found to be the CO_2 formation path, with the lowest activation barrier. However, due to high CO coverage on the Pt surface the microkinetic modeling showed that this reaction step is limited by the small OH coverage. Instead, the direct decomposition step: COOH = CO_2 + H is dominating.

The activity of a supported metal catalyst does not exclusively depend on the nature of the metal, but the support may play an active role as well. For example, the activity of WGS catalysts based on a cerium oxide support [22–26] has been ascribed to a redox mechanism, where CO_2 is formed by reduction of the cerium oxide surface with CO adsorbed on the metal and hydrogen is formed by reoxidation of the cerium oxide with water [27]. As the role of the metal in such a mechanism is different from that in a catalyst with an inactive support, it can be anticipated that the parameters controlling the WGS activity depend on the type of support that is chosen.

In order to obtain a better understanding of the water gas shift reaction over transition metals supported on different supports, we present WGS activity measurements for 12 transition metals supported on inert $MgAl_2O_4$ and redox-active $Ce_{0.75}Zr_{0.25}O_2$. Zirconium is added to the cerium oxide in order to improve the thermal stability [28]. All catalysts were produced and treated in a very similar way, in an attempt to create a consistent set of catalysts in which the differences in activity can be ascribed to the type of metal. The metals used in this series of experiments are: Fe, Co, Ni, Cu, Ru, Rh, Pd, Ag, Re, Ir, Pt and Au. The activity data are related to the adsorption energies for carbon monoxide and oxygen on the metals, and it is discussed how improved metal or alloy based WGS catalysts can be conceived. It should be pointed out that comparing a large number of catalysts for trends has the price of abandoning comparing the individually optimized catalysts. This will, however, be the subject of future work having identified the most promising metal-support systems.

2. Experimental

The $MgAl_2O_4$ support used in the present study was an industrially produced material from Haldor Topsøe A/S, with a BET surface area of 60.4 m^2/g (N_2 adsorption), a pore volume of 433 ml/kg (Hg-intrusion), and a spinel crystallite size of 133 Å, determined by X-ray diffraction (XRD). To prepare the $Ce_{0.75}Zr_{0.25}O_2$ support, 580 g $Ce(NO_3)_3{\cdot}6H_2O$ was dissolved in water to a total volume of 400 ml, and 160 g of a 70 wt.% $Zr(OCH(CH_3)_2)_4$ in 1-propanol was diluted with 2-propanol to a total volume of 600 ml. The aqueous solution was added to the alcohol solution under turbo mixing and a solid phase precipitated. The precipitate was filtered off, washed, dried and calcined at 500 °C for 5 h. The cerium and zirconium content in the calcined product are 62.8 wt.% Ce and 13.2 wt.% Zr, corresponding to a molar stoichiometry of $Ce_{0.75}Zr_{0.25}O_2$. XRD showed cubic cerium oxide with a crystallite size of 68 Å (D220), and a lattice constant of 5.39 Å, which is somewhat lower than the lattice constant for pure cerium oxide (5.41 Å), indicating incorporation of zirconium in the cerium oxide lattice [28]. The BET surface area of the material is 70 m^2/g, and the pore volume is 410 ml/kg.

All metal catalysts were prepared by incipient wetness impregnation. The support material (particle size 150–300 μm) was impregnated with an aqueous solution of the metal salts of appropriate concentrations, and a volume that equals the pore volume of the support. The following metal salts were used: $Fe(NO_3)_3{\cdot}9H_2O$, $Co(NO_3)_2{\cdot}6H_2O$, $Ni(NO_3)_2{\cdot}6H_2O$, $Cu(NO_3)_2{\cdot}2.5H_2O$, $Ru(NO)(NO_3)$, $Rh(NO_3)_3$, $Pd(NH_3)_4(HCO_3)_2$, $AgNO_3$, NH_4ReO_4, $IrCl_3{\cdot}xH_2O$, $Pt(NH_3)_4(HCO_3)_2$, and $HAuCl_4{\cdot}3H_2O$. The Re and the Ru catalysts were dried at room temperature and reduced in flowing hydrogen at 450 °C for 2 h to avoid possible formation of volatile oxide species; all other catalysts were dried at 120 °C and calcined in a

Table 1
Results for $MgAl_2O_4$ supported metals. Metal content determined by ICP. Metal particle size diameter from TEM investigations. WGS rate constant determined as described in text.

Catalyst	Metal content		Number average diameter (nm)	Standard deviation (nm)	Metal surface area[a] (m^2/g)	k at 270 °C (mmol/(mol metal s atm^2))	E_a (kJ/mol)
	wt.%	mmol/g					
Fe on $MgAl_2O_4$	1.07	0.191	–	–	–	4.0	74
Co on $MgAl_2O_4$	4.86	0.825	9.28	3.23	2.87	2.1	91
Ni on $MgAl_2O_4$	0.97	0.166	28.53	12.88	0.16	26.8	111
Cu on $MgAl_2O_4$	1.04	0.164	4.17	1.11	1.45	1509.8	44
Ru on $MgAl_2O_4$	1.70	0.168	2.74	2.56	0.56	10.5	126
Rh on $MgAl_2O_4$	1.77	0.172	1.98	1.18	2.36	98.0	86
Pd on $MgAl_2O_4$	1.83	0.172	5.61	5.29	0.45	43.2	76
Ag on $MgAl_2O_4$	1.96	0.181	3.22	2.81	1.05	9.4	57
Re on $MgAl_2O_4$	3.22	0.173	–	–	–	32.0	82
Ir on $MgAl_2O_4$	2.35	0.122	3.84	3.42	0.59	5.9	86
Pt on $MgAl_2O_4$	3.00	0.154	4.44	2.69	1.05	284.3	87
Au on $MgAl_2O_4$	3.18	0.161	3.66	1.66	1.86	25.1	34

[a] Calculated by assuming hemispherical shape of the metal particles on the support.

Table 2
Results for $Ce_{0.75}Zr_{0.25}O_2$ supported metals. Metal content determined by ICP. WGS rate constant determined as described in text.

Catalyst	Metal content		k at 270 °C (mmol/(mol metal s atm^2))	E_a (kJ/mol)
	wt.%	mmol/g		
Fe on $Ce_{0.75}Zr_{0.25}O_2$	0.78	0.140	19.4	94
Co on $Ce_{0.75}Zr_{0.25}O_2$	0.99	0.168	60.8	103
Ni on $Ce_{0.75}Zr_{0.25}O_2$	1.03	0.176	175.4	87
Cu on $Ce_{0.75}Zr_{0.25}O_2$	1.15	0.181	44.9	84
Ru on $Ce_{0.75}Zr_{0.25}O_2$	1.52	0.150	639.0	67
Rh on $Ce_{0.75}Zr_{0.25}O_2$	1.54	0.150	849.1	67
Pd on $Ce_{0.75}Zr_{0.25}O_2$	1.76	0.165	690.1	62
Ag on $Ce_{0.75}Zr_{0.25}O_2$	1.53	0.141	31.9	81
Re on $Ce_{0.75}Zr_{0.25}O_2$	2.51	0.135	1163.5	70
Ir on $Ce_{0.75}Zr_{0.25}O_2$	2.40	0.125	101.2	76
Pt on $Ce_{0.75}Zr_{0.25}O_2$	3.37	0.173	3560.0	74
Au on $Ce_{0.75}Zr_{0.25}O_2$	3.00	0.152	6.8	61

furnace at 450 °C for 2 h. The final metal contents in the catalysts, as determined by ICP, are given in Tables 1 and 2. High-Angle Annular Dark Field Scanning Transmission Electron Microscopy (HAADF-STEM) in a Philips CM-200 electron microscope and XRD were used to evaluate the metal particle size in the catalysts supported on $MgAl_2O_4$.

The WGS activity of the catalysts was determined in a setup of 10 parallel fixed-bed reactors. The reactors consisted of stainless steel tubes with an inner diameter of 6 mm, which were mounted in a single heater block and connected to a common gas inlet. The flow distribution over the reactor channels, obtained by placing flow restrictions upstream of the reactors, varied from 7 to 12% of the total flow per channel. The flow distribution, however, was stable and reproducible, and is accounted for in the data analysis. Water was evaporated into the gas stream using a syringe pump at 260 °C, just upstream of the flow distribution. To monitor the reactor exit gas, a calibrated mass spectrometer (Balzers GAM400) is sequentially connected to each reactor via a 10-position sampling valve (Valco). An empty reactor is always included to monitor the concentrations in the feed gas.

To perform the activity measurements, each reactor is filled with a 250 mg catalyst sample with a sieve fraction 150–300 μm. Prior to the activity measurements the catalysts were heated to 360 °C in a mixture of 20% CO in Ar in order to reduce and stabilize the metal particles. After this treatment, water was added to the gas feed to produce a mixture of approximately 16% CO and 16% water vapor in Ar, which is the feed gas, used in the activity measurements. The measurements were done by stepwise lowering the temperature from 360 to 210 °C in steps of 30 °C, and measure the composition of the reactor exit gas at an average flow of 150, 100, 75, 60, 50, and 40 Nml/min per reactor channel. By starting at high temperature the deactivation due to sintering of the metal particles in the measurements at lower temperatures is minimized, and a more stable behavior is obtained. The components He, Ar, O_2, H_2O, H_2, CO, CO_2, CH_4, and CH_3OH were monitored. The final concentration values are obtained from the average of 10 mass spectrometer measurements, which were collected during about 2 min for each reactor channel.

3. Results

3.1. Basis for comparison of catalytic activity

The goal of this study is to compare the water gas shift activity for 12 different transition metals on 2 different support materials, and relate the activities to the chemical nature of the transition metal. The conversion is measured with the same feed gas and at the same process conditions for all catalysts. However, it is not trivial to compare the measured activities, due to the diverse chemical nature of the catalysts, even though the all catalysts are very similar and contain about the same molar amount of metal. In the following, we briefly discuss our considerations to establish a basis for the comparison of the activity for the different catalysts.

3.1.1. Reaction kinetics

In principle, each catalyst could have its own kinetic behavior, since the reaction mechanism and intermediates that are formed may be different depending on the active metal. This means that the ranking and relative activities of the catalysts can depend on the specific conditions of the measurement, and the reaction gas used. However, since we compare the activities measured at the same feed gas and process conditions, a single kinetic expression is used for all catalysts. As a consequence, the differences in activity are reflected in the rate constants only. Evaluation of the activity with a rate equation also allows for the required integral analysis, as the experimental data cover a wide range of conversion levels. An example of this is shown in Fig. 1: the measured conversion at 270 °C and a flow of approximately 60 Nml/min, ranges from about 60% for the most active catalyst to below 1% for the least active catalysts. Moreover, we also conveniently correct for the differences in flow through the parallel reactor channels in such an analysis. Therefore, the rate constant based on a single kinetic expression is considered a better measure of the activity than the measured conversions or a differentially determined reaction rates.

3.1.2. Catalyst pretreatment

For practical reasons, the same pretreatment procedure was used for all catalysts. As mentioned in the previous section, this pretreatment comprises heating to 360 °C in a dry mixture 20% CO/Ar, followed by addition of water, which starts the WGS reaction. This pretreatment may be very suitable for some metals, while it can be less appropriate for others and we realize that the measured activity may be close to the maximum attainable activity for some metals, while it may be significantly lower for other catalysts. Therefore some differences in the trend may be observed if a different pretreatment procedure or temperature range is chosen, although the general picture is expected to hold.

3.1.3. Dispersion

The dispersion of the metal particles depends on the surface energy of the metal and the metal/support interaction energy, and therefore the above mentioned pretreatment will result in a different dispersion of the metal particles for each catalyst. Table 1 includes the measured particle size distributions, represented as an average particle size and standard deviation, and the corresponding metal surface areas of the used and passivated $MgAl_2O_4$-supported catalysts determined from HAADF-STEM images. Co, Ni, and Cu have a lower contrast in HAADF-STEM, and additional EDS mapping was used to identify the metal particles in the HAADF-STEM images. The Co, Ni, and Cu on $MgAl_2O_4$ catalysts

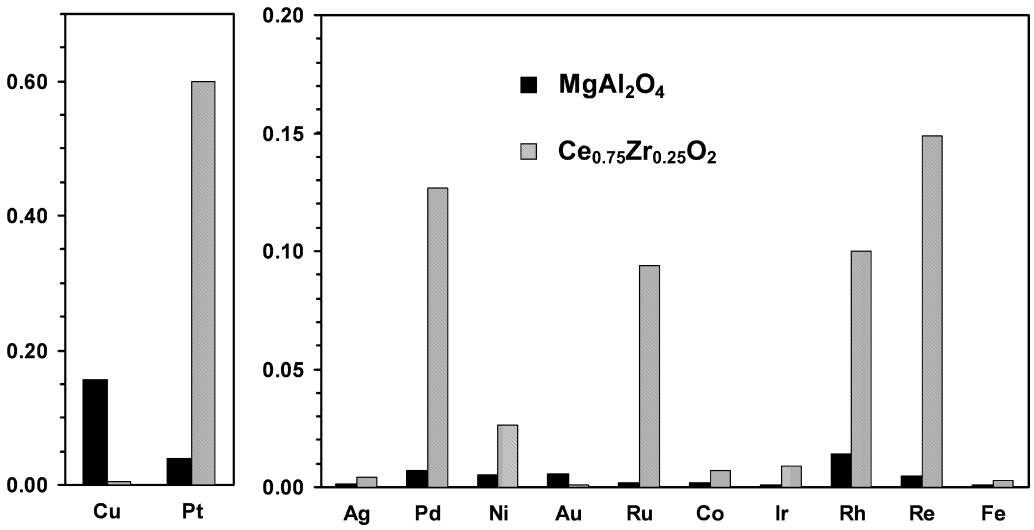

Fig. 1. Measured conversions for water gas shift at 270 °C over $MgAl_2O_4$ (black) and – $Ce_{0.75}Zr_{0.25}O_2$ (grey) – supported transition metal catalysts. Feed 16% CO, 16% H_2O in Ar. Flow approximately 60 Nml/min.

were heated to 360 °C in a gas mixture of 16% CO, 16% water in Ar for 10 h in a separate treatment, to simulate the heat treatment in the activity measurements, and transferred to the electron microscope in a protective atmosphere.

Most $MgAl_2O_4$-supported catalysts have particles in the size range 3–5 nm, and a metal surface area in the range 0.5–1.5 m^2/g. The Ni/$MgAl_2O_4$ catalyst has much larger particles, indicating significant sintering of this catalyst, possibly due to Ni-carbonyl formation during activation and use. The Rh/$MgAl_2O_4$ catalyst shows a high dispersion, indicating a lower degree of sintering of this catalyst, compared to the other catalysts. The metal particles were not detected in XRD in any of the samples, which could indicate polycrystalline metal particles.

For the $Ce_{0.75}Zr_{0.25}O_2$-supported catalysts, we did not succeed to obtain a reliable measurement of the particle sizes or dispersion. HAADF-STEM does not yield good contrast between metal particles and support, due to the high amount of Ce in the support. H_2 and CO chemisorption is complicated by the reactivity of the support towards these compounds, which result in large uncertainties, in particular for metals with a weak adsorption (Cu, Ag, Au). XRD did not show diffraction related to the metal particles, like the $MgAl_2O_4$-supported catalysts. This indicates either small or polycrystalline metal particles, or possibly some incorporation of the metals in the support [29–37]. Therefore, we find that the catalytic activity expressed per mol metal is the most reliable basis for comparing the activities of the catalysts with the different supports.

3.1.4. Oxidation state of the metals

To compare the activities in a meaningful way, it is required that the metal compounds are present in the metallic state. A simple thermodynamic analysis reveals that Fe is the only metal used with a tendency to form a bulk oxide in the reaction gas around 300 °C [14]. The measured WGS activity on the Fe catalysts is possibly due to the activity of Fe oxide, as magnetite is the active component in high temperature shift catalysts [38]. Therefore, the measured activities for the Fe catalysts may be misleading, and these data are omitted in the comparison of the activity of the different catalysts.

3.2. Determination of catalytic activity

As explained above, a single kinetic expression is used to evaluate the activity of all catalysts. A simple expression to describe the WGS reaction is obtained by assuming that the rate of the WGS reaction is first order in CO and H_2O, which results in the following rate equation:

$$r = k^{+} p_{CO} p_{H_2O} - k^{-} p_{CO_2} p_{H_2} \approx k p_{CO} p_{H_2O} \quad (2)$$

where k^+ and k^- are the rate constants for the forward and backward reactions in the WGS equilibrium, respectively, and p is the partial pressure of the indicated compound. The term for the backward reaction is ignored in the evaluation of the rate constant; its contribution is less than 1% at a conversion level of 40%, and about 5% at a conversion level of 60%.

By writing the partial pressures as the mole fraction of the total pressure, $y \cdot p_{tot}$, and expressing the mole fraction in terms of conversion, and the initial concentrations of CO and H_2O, the rate equation becomes:

$$r = y^0_{H_2O} \frac{dX}{d(W/F)} = k\, p^2_{tot} y^0_{H_2O} (1 - X)(y^0_{CO} - y^0_{H_2O} X) \quad (3)$$

W is the catalyst weight, F is the total gas flow, and p_{tot} is the total pressure at the reactor inlet.

Formation of methanol and methane, which are possible byproducts in our experiment, did not occur, and therefore the partial pressure of hydrogen can be used to measure the WGS activity. The stoichiometry of the water gas shift reaction prescribes that the consumed amounts of CO and water, and the produced amounts of CO_2 and H_2 are all equal. Our analysis is based on the measured concentration of H_2, since for hydrogen there is no signal due to the feed gas, and therefore an accurate measurement of the conversion can be obtained down to a conversion of about 0.01%. The conversion X is then determined as:

$$X = \frac{y_{H_2}}{y^0_{H_2O}} \quad (4)$$

where y_{H_2} is the measured mole fraction of hydrogen, and $y^0_{H_2O}$ is the mole fraction of water in the gas feed.

For each catalyst, the rate constant k is determined at 360, 330, 300, 270, 240, and 210 °C, using Eq. (3). The validity of the rate expression (Eqs. (2) and (3)) is corroborated by the similar k values obtained in measurements for different W/F values at the same temperature. All measured data were adequately described with an error margin in the rate constant of 20% at high conversion levels, and about 10% at low conversion levels, which is acceptable for the purpose of the present study. Choi and Stenger have also shown that, in the case of the WGS reaction over a $Cu/ZnO/Al_2O_3$ catalyst, the difference between more complicated rate expressions and the

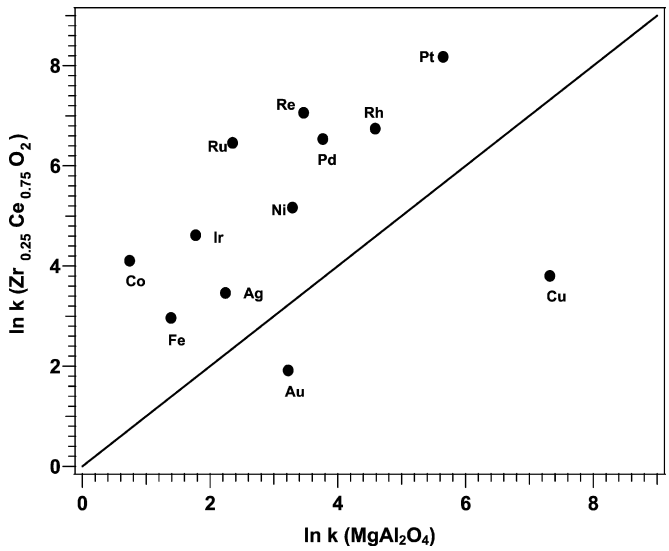

Fig. 2. Comparison of activities at 270 °C for $MgAl_2O_4$ and $Ce_{0.75}Zr_{0.25}O_2$-supported catalysts. The rate constant k is expressed in mmol/(mol metal s atm^2). The solid line indicates equal activity. Cu and Au are below the line, indicating that the activity on the $MgAl_2O_4$ support is higher than on the $Ce_{0.75}Zr_{0.25}O_2$ support; all other catalysts are more active on the $Ce_{0.75}Zr_{0.25}O_2$ support.

simple expression in Eq. (3) [39], suggesting that Eq. (3) equation is a good approximation for WGS kinetics.

3.3. Water gas shift activity

The trends observed in the activity for the different metals are very similar for all the temperatures investigated; we use the rate constants at 270 °C to identify the trends and these values are also included in Tables 1 and 2. Cu is the most active metal on the $MgAl_2O_4$-supported; and the measured activities follow the order of Cu > Pt > Rh > Pd > Re > Ni > Au > Ru ∼ Co ∼ Ag > Ir (∼Fe) at 270 °C when the rate constant is measured in mmol/(mol metal s atm^2). For the $Ce_{0.75}Zr_{0.25}O_2$-supported catalysts, Pt is the most active metal, and the activity follows the order of Pt > Re > Rh ∼ Pd > Ru > Ni > Ir ∼ Co > Cu > Ag (>Fe) > Au. This agrees very well with the trend found by Radhakrishnan et al. [40]. These trends are also visible in the measured conversions shown in Fig. 1. We also find that the activity of the $Ce_{0.75}Zr_{0.25}O_2$-supported catalysts generally is higher than for the $MgAl_2O_4$-supported catalysts; only Cu and Au show the opposite effect. This result is visualized in Fig. 2, which displays the activity for the metal compounds on the $Ce_{0.75}Zr_{0.25}O_2$ support as a function of the activity on the $MgAl_2O_4$ support. The Cu and Au lie below the line that indicates equal activity; all other metals are above the line.

The apparent activation energies for the catalysts are determined from the Arrhenius relation, using only results with a measured conversion below 40% to avoid inaccuracies due to the approach to equilibrium. The activation energies for all $Ce_{0.75}Zr_{0.25}O_2$-supported catalysts are in the range 60–100 kJ/mol. For the $MgAl_2O_4$-supported catalyst we find a higher activation energy for Ni and Ru, and a noticeable lower activation energy for Cu/$MgAl_2O_4$ (45 kJ/mol) and Au (34 kJ/mol).

4. Discussion

4.1. WGS activity of $MgAl_2O_4$-supported catalysts

To relate the water gas shift activity with the chemical properties of the transition metal, the relevant properties that determine that activity must be identified. Schumacher et al. [16] have proposed that the activity of the transition metal catalysts can be described by the adsorption energy of CO (ΔE_{CO}) and oxygen (ΔE_O), the latter also representing the interaction of water with the metal surface. The COOH surface species, recently found to be a reaction intermediate [22,23], was not included in the analysis that lead to this conclusion, but as COOH binds to the surface via the C atom like CO it is our assumption that ΔE_{CO} is also a good descriptor for the adsorption energy of COOH. Fig. 3 shows the water gas shift activity of the $MgAl_2O_4$-supported catalysts as a function of the adsorption energy of CO (top) and oxygen (bottom). The adsorption energies for step sites on the pure metals, obtained from DFT calculations [41], are used; the values are given in Table 3. The adsorption energies at step sites are chosen for two reasons. First, it is likely that the step sites, and not the terrace sites, are the most active sites for the WGS reaction, since the step sites are generally more reactive [42]. Secondly, by using the adsorption energies for step sites, the influence of the crystal structure of the metal (fcc, bcc, or hcp) is reduced, since the step sites on different crystal faces are more similar to each other than the low index planes. Since the adsorption energies of CO and O on step sites of Re are not known, this metal is omitted; Fe is omitted, since it probably is oxidized under the conditions of the activity measurement (see Section 3.1).

It is clear from Fig. 3, that a comparison of the WGS activity with the adsorption energy of CO on transition metals (top panels) result in a somewhat less clear correlation for the $MgAl_2O_4$-supported catalysts. The CO adsorption energy is apparently not a good descriptor for the WGS activity of transition metals supported on $MgAl_2O_4$: Cu and Pt are the two most active metals, but the adsorption energy of CO is very different on these metals. This is clearly different from the findings of Grenoble et al. [14], who obtained volcano-type relationship between WGS activity and CO chemisorption energy for Al_2O_3-supported catalysts. The volcano-shaped curve in that work, however, is mainly based on the large metal particle size for Cu and, consequently, a very high turn-over frequency, as compared to the other metals, which we do not find to the same extent.

In the bottom panels of Fig. 3, the WGS activity of the $MgAl_2O_4$-supported metals is compared to the dissociative adsorption energy of oxygen, ΔE_O. This results in a volcano-shaped curve with a maximum around $\Delta E_O = -2.5$ eV. This suggests that ΔE_O is an appropriate descriptor for the WGS activity for transition metals, pointing to the activation of water as the property that determines WGS activity. A correction for the dispersion of the metal, shown in the right panels in Fig. 4, does not change the observed trends in a significant way, although the ranking of the metals changes.

An interpretation of this volcano-type relation is that the metals with oxygen adsorption energy below 2.5 eV have a low activity due to a low rate for dissociation of water, and the metals with higher oxygen adsorption energy are poisoned by surface species binding to the surface via oxygen atoms, e.g. OH and oxygen [16]. The rate of the WGS reaction, however, also depends on the coverage of CO, which can be very different for the different metals. This is

Table 3
Values for the adsorption energy of atomic oxygen and molecular CO obtained from DFT calculations [41].

Element	ΔE_O (eV)	ΔE_{CO} (eV)
Co	−5.07	−1.50
Ni	−3.90	−1.66
Cu	−2.51	−0.62
Ru	−4.62	−1.77
Rh	−4.03	−1.79
Pd	−1.20	−1.74
Ag	−0.65	−0.06
Ir	−4.65	−1.96
Pt	−2.17	−1.89
Au	0.54	−0.35

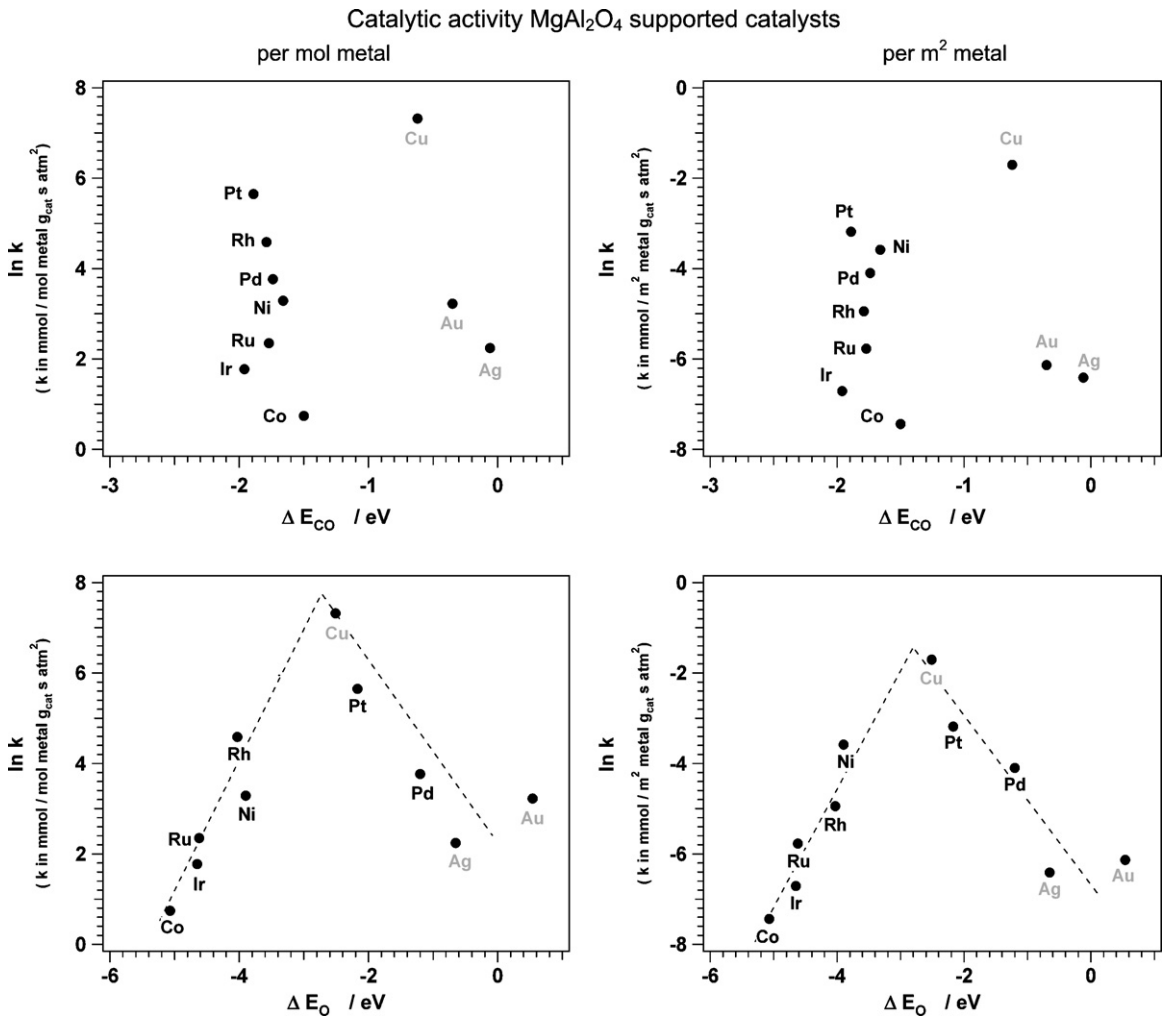

Fig. 3. *Left panels*: Activity ($\ln k$, k in mmol/(mol metal s atm^2)) of the $MgAl_2O_4$-supported catalysts at 270 °C as a function of the adsorption energy of carbon monoxide, E_{CO} (top) and atomic oxygen, E_O (bottom). A correction for dispersion (right half) largely results in the same trend.

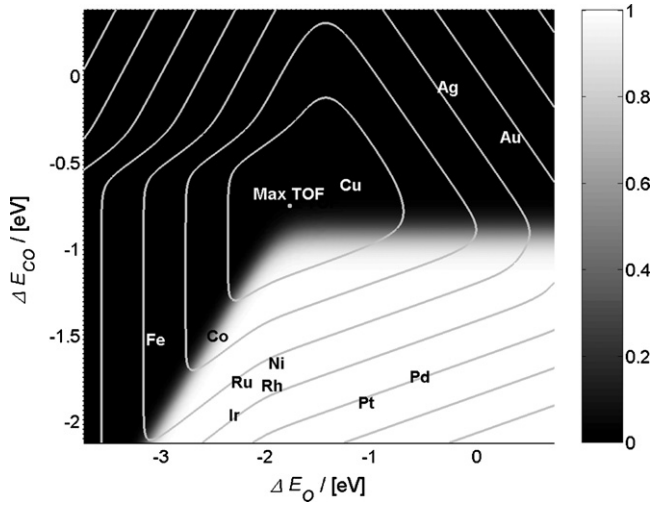

Fig. 4. Surface coverage of carbon monoxide (represented by grey scale) at varying adsorption energies of oxygen and carbon monoxide relative to values for Cu as predicted by the kinetic model developed by Schumacher et al. [16] that describe the water gas shift reaction over transition metals. The turn-over frequencies are superimposed as contour lines (iso-TOF lines) and the position for the maximum shown. The corresponding energy coordinates for the included metals are marked. Conditions are $p = 1.02$ bar and $T = 270$ °C. The feed gas composition is 0.15 bar CO, 0.01 bar CO_2, 0.01 bar H_2, 0.15 bar H_2O, and 0.7 bar Ar.

illustrated in Fig. 4, which displays the estimated CO coverage at 270 °C and 1.02 bar for a gas mixture that resembles that used in our experiments. Clearly, the Cu, Au, and Ag catalysts show a low CO coverage, which is consistent with their significantly lower CO chemisorption energy, whereas all other metals, which all have a high CO chemisorption energy, show a high CO coverage. The metals on the left side of the volcano-plot in Fig. 3, Co, Ir, Ru, Rh, and Ni, all belong to the metals with a high CO coverage, and therefore the low activity for these metals could be lower due to a surface poisoning by CO as well.

If we consider the WGS activity for the metals with a high CO coverage separately, again a volcano-type relation is found with an optimum around $\Delta E_O = -3$ eV for these metals. The metals with a low CO coverage (Cu, Au, and Ag) are all to the right of the maximum, and the WGS activity increases with increasing oxygen adsorption strength. Since the activities for the metals with a weak oxygen adsorption (Cu, Au, Ag, Pt, and Pd) all seem to follow the same line, it could be argued that the CO adsorption energy does not play a significant role for the WGS activity for these catalysts. The metals investigated here do not include a metal or alloy with a weak CO chemisorption and a stronger oxygen adsorption. This would result in a higher surface coverage of OH and oxygen species, while the coverage of CO remains low, preventing CO poisoning. It can be speculated that such a metal would show an improved WGS activity compared to Cu [16].

The metals with a weak CO adsorption strength (Cu, Au, and Ag) also show a low activation energy compared to the other metals (see Table 1). The lower activation energy can actually be understood from a low surface coverage of CO on these metals. In a Langmuir–Hinshelwood type of model, a term $(1+K_{CO}p_{CO})^{-n}$ is included in the rate expression to account for surface coverage of CO [43]; where K_{CO} is the equilibrium constant for CO adsorption, p_{CO} is the partial pressure of CO and n the number of sites involved in the rate limiting step. At low CO coverage, the term $K_{CO}p_{CO}$ becomes very small, and can be neglected. At high CO coverages, the term is approximately equal to $(K_{CO}p_{CO})^{-n}$, which results in a contribution to the apparent activation energy of $-n\Delta H_{CO}$. This means an increase in the apparent activation energy, since the adsorption enthalpy of CO, ΔH_{CO}, is a negative number. Therefore, the activation energy for WGS is expected to be higher for metals with a high coverage of CO, in full agreement with the activation energies found in the present study. This simple analysis, however, overestimates the effect of CO adsorption, since it does not include the coverage dependent CO adsorption strength, due to the repulsive interaction between the adsorbed CO molecules [26,44–46] and explains why the apparent activation energies for the metals with high CO coverage is not as high at the simple Langmuir–Hinshelwood analysis suggest.

The order of activity for $MgAl_2O_4$-supported catalysts found in this study is Cu > Pt > Ni > Pd > Rh > Ru > Au > Ag > Ir > Co (corrected for dispersion). The ranking found by Grenoble et al. for Al_2O_3-supported catalysts is Cu > Co > Ru > Ni > Pt > Au > Fe > Pd > Rh > Ir. Clearly, Cu is found to be active in both studies, and Ir is inactive in both studies. In contrast to Grenoble et al., we find a high activity for Pt and Pd, and a low activity for Co. These differences are possibly related to the different support material, the activation procedure, or the specific conditions at which the activity was measured. The ranking found by Schumacher et al., based on correlations between activation energy and the adsorption energies for CO and O, is Cu > Co > Ru > Fe > Ni > Rh > Au > Ir > Pd > Pt, if adsorption energies at steps are used [16]. If adsorption energies on terraces are used, they find Cu > Ni > Pt > Rh > Ru > Au > Ir > Pd. Note that the ranking in the last series is almost the same as ours; only the measured activity of Pd is higher than expected from Schumacher's model. The measured activity for the $Co/MgAl_2O_4$ catalyst is much lower than expected from Schumacher's model.

4.2. WGS activity of $Ce_{0.75}Zr_{0.25}O_2$-supported catalysts

The observed trends for the $Ce_{0.75}Zr_{0.25}O_2$-supported catalysts are quite different from those observed on the $MgAl_2O_4$-supported catalysts. The $Pt/Ce_{0.75}Zr_{0.25}O_2$ catalyst is the most active one, and Cu is actually one of the least active metals on this support. This clearly indicates that the support is an important factor in understanding the WGS activity of metal catalysts, and therefore a characterization of the metal phase alone is not (always) sufficient.

Fig. 5 shows the water gas shift activities for the transition metals supported on $Ce_{0.75}Zr_{0.25}O_2$ as a function of the adsorption energies for carbon monoxide and oxygen, similar to Fig. 3. Reliable data for the metal dispersion on the $Ce_{0.75}Zr_{0.25}O_2$ support are not available, and therefore we use only the activity per mol metal here. Due to the relative low activity of Cu, we do not find a clear volcano-shaped relationship between the binding energy of oxygen and the WGS activity as we did for the $MgAl_2O_4$-supported catalyst, so it seems that the CO binding energy is a better descriptor for the WGS activity of the $Ce_{0.75}Zr_{0.25}O_2$-supported catalysts. If this interpretation is valid, it shows, that the parameter that controls the WGS activity of the metal actually can change when different support materials are used: The WGS activity of $Ce_{0.75}Zr_{0.25}O_2$-supported metals is best understood from the adsorption energy of CO on the metal (E_{CO}),

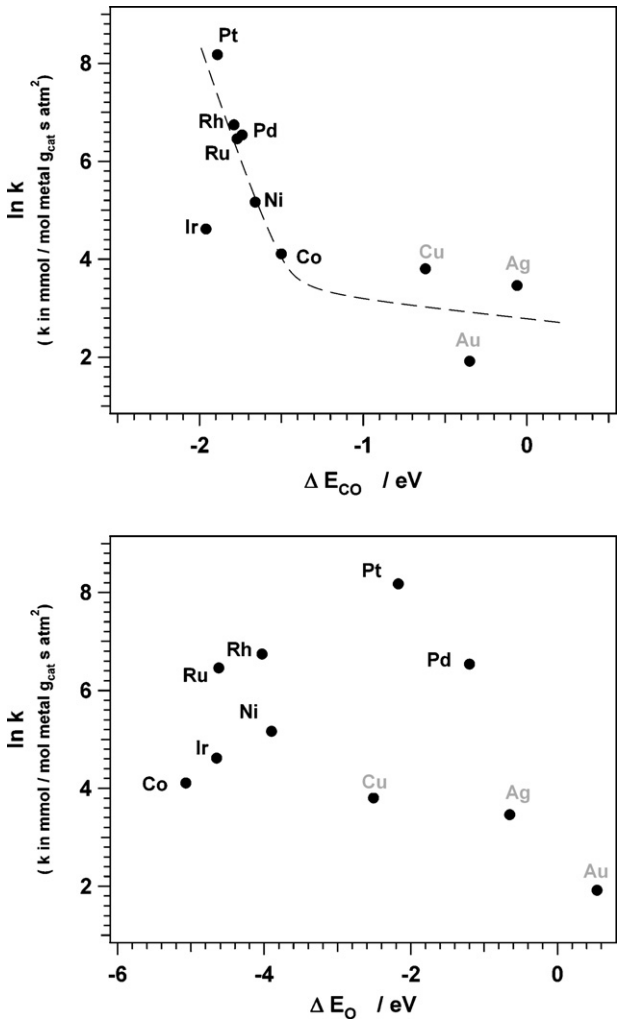

Fig. 5. Activity ($\ln k$, k in mmol/(mol metal s atm^2)) for the $Ce_{0.75}Zr_{0.25}O_2$-supported catalysts at 270 °C as a function of the adsorption energy of carbon monoxide, ΔE_{CO} (top panel) and atomic oxygen, ΔE_O (bottom panel).

while the adsorption energy of oxygen (E_O) seems more important if a $MgAl_2O_4$ support is used.

It should be noted that removing the Cu data points from all the plots makes the difference between the WGS trends for two supports very small. However, there is no good reason to neglect the Cu data. As already mentioned in the introduction recent detailed studies did not find a different reaction mechanism for Cu compared to Pt [20,21], which is important since the different activity of these two metals is important for rejecting the adsorption energy of O as a good activity-descriptor for $Ce_{0.75}Zr_{0.25}O_2$-supported catalysts. Another possible reason for disregarding the Cu data in Fig. 5 could be a very low dispersion of the Cu on $Ce_{0.75}Zr_{0.25}O_2$ catalyst, but this is unlikely since no Cu related peaks were observed in the XRD spectra.

The top panel in Fig. 5 shows that the most active metals on $Ce_{0.75}Zr_{0.25}O_2$ have a strong adsorption to CO, and therefore a high CO coverage under WGS conditions (Fig. 4). From the trend line in Fig. 5, one could expect that an improved WGS activity can be obtained by using a $Ce_{0.75}Zr_{0.25}O_2$-supported metal or alloy with a stronger CO adsorption than Pt. A Pt/Re alloy on a cerium–zirconium oxide support – the two most active metals found for this support in this study – is possibly an example: the alloy is more active than pure Pt [47], and DFT calculations indicate that the binding energy of CO on Re is higher than on Pt [48], which suggests a higher CO adsorption energy on the alloy as well.

A possible explanation for a change in the best activity-descriptor from E_O for $MgAl_2O_4$-supported catalysts to E_{CO} for the $Ce_{0.75}Zr_{0.25}O_2$-supported is that the $MgAl_2O_4$ support is inactive, while the dissociation of water can occur on the (redox active) $Ce_{0.75}Zr_{0.25}O_2$ support [49,50], similar to the role of Ce oxide in oxidation reactions [34,51] or dry reforming [52]. In such a scenario, a high CO coverage on the metal particles does not block the water dissociation reaction, and is therefore beneficial for the WGS activity. Since the water dissociation does not take place on the metal particles, a clear correlation between oxygen binding energy and WGS activity is not expected, in full agreement with our findings (Fig. 5, bottom panel). This explanation is also consistent with the observation the activity for the $Ce_{0.75}Zr_{0.25}O_2$-supported catalysts is significantly higher for the metals with a strong CO adsorption, but about the same or lower for the metals with a weak CO adsorption (Cu, Ag, Au) (see Fig. 2). Finally, the volcano-shaped correlation between oxygen binding energy and WGS activity on $MgAl_2O_4$-supported catalysts suggests that the WGS activity is determined by the catalyst's ability to dissociate water or accommodate adsorbed O. Since this reaction on the $Ce_{0.75}Zr_{0.25}O_2$ support takes place on the support, and not on the metal, the activation energy of $Ce_{0.75}Zr_{0.25}O_2$-supported catalysts becomes less dependent on the metal. This is what we have found here: For the $Ce_{0.75}Zr_{0.25}O_2$-supported catalysts, the activation energies are in the range 60–100 kJ/mol, including that of the Cu and Au catalyst, while the activation energies for the $MgAl_2O_4$-supported Cu and Au catalysts are clearly lower.

5. Conclusion

The water gas shift activity of 12 different transition metals supported on $MgAl_2O_4$ spinel and $Ce_{0.75}Zr_{0.25}O_2$ has been determined. All catalysts contained approximately the same molar amount of metal, and were prepared and treated in a very similar way. The observed trends in activity are different for the two supports: on $MgAl_2O_4$ spinel, Cu is the most active catalyst, followed by Pt, Rh, Pd, and Ni. On the $Ce_{0.75}Zr_{0.25}O_2$, the most active catalyst is Pt, followed by Re, Rh, and Pd, while Cu is among the least active catalysts.

To understand the observed trends in water gas shift activity for the different metals, the measured activities were correlated with the adsorption energy of CO and oxygen on the different metals; the latter is also a measure for the stability of OH on the metal surfaces. For the $MgAl_2O_4$-supported catalysts, the maximum activity is found for metals with a binding energy of oxygen around −2.5 eV, while no clear correlation exists with the adsorption energy of CO. The opposite is observed for the $Ce_{0.75}Zr_{0.25}O_2$-supported catalysts; the activity increases with increasing adsorption strength for CO, and does not depend on the adsorption of oxygen. This change in activity-descriptor for the different supports can be rationalized by the possibility that water dissociation occurs on the redox-active $Ce_{0.75}Zr_{0.25}O_2$ support, whereas the $MgAl_2O_4$ support is inactive. This also implies that there a single parameter that describes the water gas shift activity of a metal in general does not exist, the role of the support has to be taken into account, and consequently, the best choice of metal for a WGS catalyst depends on the support. The present study suggests that a metal or alloy that is more reactive towards oxygen, compared to Cu is beneficial with the $MgAl_2O_4$ support while a metal or alloy with stronger CO bond than that on Pt should be used with the $Ce_{0.75}Zr_{0.25}O_2$ support.

References

[1] R. Farrauto, S. Hwang, L. Shore, W. Ruettinger, J. Lampert, T. Giroux, Y. Liu, O. Ilinich, Ann. Rev. Mater. Res. 33 (2003) 1.
[2] K. Kochloefl, in: G. Ertl, H. Knözinger, J. Weitkamp (Eds.), Water Gas Shift and COS Removal, Handbook of Heterogenous Catalysis, vol. 4, VCH, Weinheim, 1997, p. 1831.
[3] C. Hardacre, A.A. Foncesca, R. Burch, Y. Chen, J. Fisher, A. Goguet, P. Hu, R.W. Joyner, B.S. Mun, D. Thompsett, D. Tibiletti, Stud. Surf. Sci. Catal. 172 (2007) 269.
[4] S.M. Opalka, T.H. Vanderspurt, R. Radhakrishnan, Y. She, R.R. Willigan, J. Phys.: Condens. Matter 20 (2008), 064237-064237/12.
[5] A. Haryanto, S. Fernando, S. Adhikari, Catal. Today 129 (2007) 269.
[6] C.H. Kim, L.T. Thompson, J. Catal. 244 (2006) 248.
[7] W. Deng, M. Flytzani-Stephanopoulos, Angew. Chem. Int. Ed. 45 (2006) 2285.
[8] D. Tibiletti, A. mieiro-Fonseca, R. Burch, Y. Chen, J.M. Fisher, A. Goguet, C. Hardacre, P. Hu, D. Thompsett, J. Phys. 109 (2005) 22553.
[9] S.Y. Choung, M. Ferrandon, T. Krause, Catal. Today 99 (2005) 257.
[10] C.H. Kim, L.T. Thompson, J. Catal. 230 (2005) 66.
[11] X. Liu, W. Ruettinger, X. Xu, R. Farrauto, Appl. Catal. B 56 (2005) 69.
[12] M.P. Andersson, T. Bligaard, A. Kustov, K.E. Larsen, J. Greeley, T. Johannessen, C.H. Christensen, J.K. Nørskov, J. Catal. 239 (2006) 501.
[13] C.J.H. Jacobsen, S. Dahl, B.S. Clausen, S. Bahn, A. Logadottir, J.K. Nørskov, J. Am. Chem. Soc. 123 (2001) 8404.
[14] D.C. Grenoble, M.M. Estadt, D.F. Ollis, J. Catal. 67 (1981) 90.
[15] P. Sabatier, La catalyse en chimique organique, Bérange, Paris, 1920.
[16] N. Schumacher, A. Boisen, S. Dahl, A.A. Gokhale, S. Kandoi, L.C. Grabow, J.A. Dumesic, M. Mavrikakis, I. Chorkendorff, J. Catal. 229 (2005) 265.
[17] C.V. Ovesen, P. Stoltze, J.K. Nørskov, C.T. Campbell, J. Catal. 134 (1992) 445.
[18] G. Jones, T. Bligaard, F. Abild-Pedersen, J.K. Nørskov, J. Phys.: Condens. Matter 20 (2008) 64239.
[19] H. Falsig, B. Hvolbæk, I.S. Kristensen, T. Jiang, T. Bligaard, C.H. Christensen, J.K. Nørskov, Angew. Chem. Int. Ed. 47 (2008) 4762.
[20] A.A. Gokhale, J.A. Dumesic, M. Mavrikakis, J. Am. Chem. Soc. 130 (4) (2008) 1402–1414.
[21] L.C. Grabow, A.A. Gokhale, S.T. Evans, J.A. Dumesic, M. Mavrikakis, J. Phys. Chem. C 112 (12) (2008) 4608–4617.
[22] P. Panagiotopoulou, D.I. Kondarides, J. Catal. 225 (2004) 327.
[23] P. Panagiotopoulou, D.I. Kondarides, Catal. Today 112 (2006) 49.
[24] R.J. Gorte, S. Zhao, Catal. Today 104 (2005) 18.
[25] Q. Fu, S. Kudriavtseva, H. Saltsburg, M. Flytzani-Stephanopoulos, Chem. Eng. J. 93 (2003) 41.
[26] A.A. Phatak, N. Koryabkina, S. Rai, J.L. Ratts, W. Ruettinger, R.J. Farrauto, G.E. Blau, W.N. Delgass, F.H. Ribeiro, Catal. Today 123 (2007) 224.
[27] T. Bunluesin, R.J. Gorte, G.W. Graham, Appl. Catal. B 15 (1998) 107.
[28] C.E. Hori, H. Permana, K.Y.S. Ng, A. Brenner, K. More, K.M. Rahmoeller, D. Belton, Appl. Catal. B 16 (1998) 105.
[29] V. Aguilar-Guerrero, B.C. Gates, Chem. Commun. (2007) 3210.
[30] A. Gayen, T. Baidya, K. Biswas, S. Roy, M.S. Hegde, Appl. Catal. A 315 (2006) 135.
[31] P. Bera, A. Gayen, M.S. Hegde, N.P. Lalla, L. Spadaro, F. Frusteri, F. Arena, J. Phys. 107 (2003) 6122.
[32] Y. Chen, L. Dong, Y.S. Jin, B. Xu, W. Ji, Stud. Surf. Sci. Catal. 101 (1996) 1293.
[33] G. Wrobel, C. Lamonier, A. Bennani, A. D'Huysser, A. Aboukaïs, J. Chem. Soc. Faraday Trans. (1996) 2001.
[34] C. de Leitenburg, A. Trovarelli, J. Catal. 156 (1995) 171.
[35] Q. Fu, W. Deng, H. Saltsburg, M. Flytzani-Stephanopoulos, Appl. Catal. B 56 (2005) 57.
[36] W. Deng, J. De Jesus, H. Saltsburg, M. Flytzani-Stephanopoulos, Appl. Catal. A 291 (2005) 126.
[37] V. Shapovalov, H. Metiu, J. Catal. 245 (2007) 205.
[38] M.V. Twigg, Catalyst Handbook, Wolfe Scientific Texts, London, 1989.
[39] Y. Choi, H.G. Stenger, J. Power Sources 124 (2003) 432.
[40] R. Radhakrishnan, R.R. Willigan, Z. Dardas, T.H. Vanderspurt, AIChE J. 52 (2006) 1888.
[41] T. Bligaard, J.K. Nørskov, S. Dahl, J. Matthiesen, C.H. Christensen, J. Sehested, J. Catal. 224 (2004) 206.
[42] J.K. Nørskov, T. Bligaard, A. Logadottir, S. Bahn, L.B. Hansen, M. Bollinger, H. Bengaard, B. Hammer, Z. Sljivancanin, M. Mavrikakis, Y. Xu, S. Dahl, C.J.H. Jacobsen, J. Catal. 209 (2002) 275.
[43] C.N. Satterfield, Rates and Kinetic Models of Catalytic Reactions, Heterogeneous Catalysis in Practice, McGraw-Hill Book Company, New York, 1980, p. 42.
[44] Y.Y. Yeo, L. Vattuone, D.A. King, J. Chem. Phys. 106 (1997) 392.
[45] S.R. Longwitz, J. Schnadt, E.K. Vestergaard, R.T. Vang, E. Lægsgaard, I. Stensgaard, H. Brune, F.J. Besenbacher, Phys. Chem. B 108 (2004) 14497.
[46] J.C. Davies, R.M. Nielsen, L.B. Thomsen, I. Chorkendorff, A. Logadottir, Z. Lodziana, J.K. Nørskov, W.X. Li, B. Hammer, S.R. Longwitz, J. Schnadt, E.K. Vestergaard, R.T. Vang, F. Besenbacher, Fuel Cells 4 (2004) 309.
[47] R. Radhakrishnan, R.R. Willigan, Z. Dardas, T.H. Vanderspurt, Appl. Catal. B 66 (2006) 23.
[48] F. Abild-Pedersen, M.P. Andersson, Surf. Sci. 601 (2007) 1747.
[49] G. Jacobs, E. Chenu, P.M. Patterson, L. Williams, D. Sparks, G. Thomas, B.H. Davis, Appl. Catal. A 258 (2004) 203.
[50] G. Jacobs, U.M. Graham, E. Chenu, P.M. Patterson, A. Dozier, B.H. Davis, J. Catal. 229 (2005) 499.
[51] R.H. Nibbelke, M.A.J. Campman, J.H.B.J. Hoebink, G.B. Marin, J. Catal. 171 (1997) 358.
[52] B.J. Liaw, Y.T. Chen, Y.Z. Chen, J. Chin. Inst. Chem. Eng. 36 (2005) 253.